Collective dynamics of pedestrians in a corridor: An approach combining social force and Vicsek models

Juan Cruz Moreno,[1,2,3] M. Leticia Rubio Puzzo,[4,5,6] and Wolfgang Paul[7]

[1]*Departamento de Ciencia y Tecnología, Universidad Nacional Quilmes, B1876BXD Quilmes, Argentina*
[2]*Consejo Nacional de Investigaciones Científicas y Tecnológicas (CONICET), C1425FQB CABA, Argentina*
[3]*Ingeniería en Informática, Departamento de Tecnología y Administración, Universidad Nacional de Avellaneda, B1868BND Avellaneda, Argentina*
[4]*Instituto de Física de Líquidos y Sistemas Biológicos (IFLYSIB), CONICET and Universidad Nacional de La Plata, Calle 59 no. 789, B1900BTE La Plata, Argentina*
[5]*CCT CONICET La Plata, Consejo Nacional de Investigaciones Científicas y Técnicas, B1904CMC La Plata, Argentina*
[6]*Departamento de Física, Facultad de Ciencias Exactas, Universidad Nacional de La Plata, 1900 La Plata, Argentina*
[7]*Institut für Physik, Martin-Luther-University Halle-Wittenberg, 06099 Halle, Germany*

(Received 19 November 2019; revised 11 July 2020; accepted 17 July 2020; published 12 August 2020)

We study the pedestrian motion along a corridor in a nonpanic regime, as usually happens in evacuation scenarios in, e.g., schools, hospitals, or airports, by means of Monte Carlo simulations. We present a model, a combination of the well-known social force model (SFM) and Vicsek model (VM), that takes into account both model interactions, based on the relative position (SFM) and based on the velocity of the particles with some randomness (modulated by an external control parameter, the noise η, VM), respectively. To clarify the influence of the model ingredients we have compared simulations using (a) the pure Vicsek model (VM) with two boundary conditions (periodic and bouncing back) and with or without desired direction of motion, (b) the social force model (SFM), and (c) the model (SFM + VM). The study of steady-state particle configurations in the VM with confined geometry shows the expected bands perpendicular to the motion direction, while in the SFM and SFM + VM particles order in stripes of a given width w along the direction of motion. The results in the SFM + VM case show that $w(t) \simeq t^{\alpha}$ has a diffusivelike behavior at low noise η (dynamic exponent $\alpha \approx 1/2$), while it is subdiffusive at high values of external noise ($\alpha < 1/2$). We observe the well-known order-disorder transition in the VM with both boundary conditions, but the application of a desired direction condition inhibits the existence of disorder as expected. Similar behavior is observed in the SFM case. For the SFM + VM case we find a susceptibility maximum which slowly increases with system size as a function of noise strength. This might be indicative of a order-disorder transition in the range of densities ($\rho\epsilon\,[\frac{1}{12}, \frac{1}{9}]$) and speeds ($v_0\epsilon$ [0.5, 2]) studied.

DOI: 10.1103/PhysRevE.102.022307

I. INTRODUCTION

Collective behavior of a large number of self-propelled particles (SPP) can result in spontaneously developing ordered motion observable by changes in adequate control parameter(s). Many groups of living beings (from cells and bacteria to fish, birds, mammals and even humans) exhibit this specific kind of motion under particular conditions. From the point of view of statistical physics, the occurrence of collective motion is a nonequilibrium phase transition which has attracted much attention of the community in the last decades (for more details see the reviews [1–3]).

The first step in the understanding of this complex behavior has been to propound simple but nontrivial models, such as the Vicsek model (VM) [4] in the middle of the nineties. In the VM, point particles with constant speed interact with eachother only by trying to align their direction of motion with their nearest neighbors, with an uncertainty of this process represented by an external noise η. This simple rule (explained in detail in Sec. II A) is enough to reproduce flocking behavior at low values of η, as commonly observed in nature.

However, the complexity of collective motion often requires to go beyond a point particle model by taking into account short- and long- range particle-particle interactions and interactions with the environment. In particular, it is possible to model a crowd as a system of particles by considering person-person and person-wall interactions. One of the first models of this type proposed to describe pedestrian motion was the so-called *social force model* (SFM) [5]. Unlike the simplistic Vicsek model, the SFM introduces the idea of social interactions by modeling the individual reaction to the effect of environment (either other pedestrians or borders), and a preferential direction of motion. This model will be explained in detail in Sec. II B.

The main idea of our work is to analyze—by using statistical mechanical tools—the evacuation of people along a hallway in a nonpanic regime, such as occurs in schools, hospitals or airports. To model this situation, it is important to take into account a series of considerations such as: the excluded-volume and mass of human-particles; the interpersonal interactions that make them want to keep their own space; the intent to remain away from the walls; the existence

of a desired direction of motion; but also the idea of being influenced by the motion of nearest neighbors. With this in mind, we propose in the present work a an approach by introducing a model—a combination of the standard VM and SFM—which takes into account position based particle interactions as in the SFM and additionally a Vicsek-like alignment modulated by a noise η. We call this the $SFM + VM$ model, and it will be described in detail in Sec. II C.

To identify the influence of the different parts of the model, we have compared the VM, the SFM + VM, and the SFM in the stationary configuration of N particles moving through a corridorlike system in a normal evacuation situation (slow speed regime). We have studied all models under the same external conditions (number of particles N, system-size $L_x \times L_y$, particle speed v_0, external noise η where applicable, etc.). In particular, we have analyzed the VM under different boundary conditions, with the purpose of introducing the effect of walls into the VM, and the idea of a desired direction of motion, such as it is defined in the SFM, to flesh out the comparison between models, and we have studied the effect of these variations on a possible order-disorder phase transition. Finally, it is worth mentioning that even though the SFM has been widely studied (see for example [6,7] and references therein), the statistical physics issues related to phase transitions of social models have been less extensively studied (see e.g. [8,9]).

The paper is organized as follows: after this introduction, a detailed description of the models can be found in Sec. II, the simulation details are presented in Sec. III, and results are analyzed and discussed in Sec. IV. In Sec. V we present a comparison to experimental findings. Finally, a summary and our conclusions are developed in Sec. VI.

II. MODELS

A. Vicsek model (VM)

The Vicsek model [4] describes the dynamics of N SPP characterized at time t by their position $\mathbf{r}_i(t)$ and velocity $\mathbf{v}_i(t)$ $(i = 1, ..., N)$, and in its simplest version all particles are considered to have the same speed v_0 ($|\mathbf{v}_i| = v_0$). At each time step, particle i assumes the average direction of motion of its neighbors (within an interaction circle of radius R_0) distorted by the existence of an external noise of amplitude η ($\eta = [0, 1]$). The simple update rules in the 2D case are given by

$$\theta_i(t + \Delta t) = \langle \theta(t) \rangle_{R_0} + \eta \xi_i(t), \tag{1}$$

$$\mathbf{v}_i(t + \Delta t) = v_0[\cos\theta_i(t + \Delta t), \sin\theta_i(t + \Delta t)], \tag{2}$$

$$\mathbf{r}_i(t + \Delta t) = \mathbf{r}_i(t) + \Delta t\ \mathbf{v}_i(t + \Delta t), \tag{3}$$

where $\langle \theta(t) \rangle_{R_0}$ is the average of the direction of motion of all the nearest neighbors of the $i-$th particle (whose distance $\|r_j - r_i\| \leqslant R_0$), and $\xi_i(t)$ is a scalar noise uniformly distributed in the range $[-\pi, \pi]$. The update rules given by Eqs. (1) and (3) are known in the literature as *angular noise* [4] and *forward update* [10], respectively. The VM has no intrinsic length and time scales, so one typically chooses $\Delta t = 1$ as the time unit and $R_0 = 1$ as the length unit. For the joined model, however, both acquire physical units through integration with the SFM. We will see that this yields the identification $\Delta t = 0.1$ s and $R_0 = 1$ m (see Sec. II C). The only control parameters of the model are the noise amplitude η, the speed v_0 and the density of particles $\rho = N/V$, where $V = L_x \times L_y$ is the volume of the 2D system.

These simple rules are enough to reproduce a fundamental aspect of collective behavior: the existence of a phase transition between a disordered state and an ordered phase (where the direction of motion is the same for all particles) as the noise intensity η decreases. The normalized average velocity of the system, defined as

$$\varphi \equiv \frac{1}{N v_0} \left| \sum_{i=1}^{N} \mathbf{v}_i \right|, \tag{4}$$

is the appropriate order parameter to describe this phase transition [2,4]. In the disordered phase $\varphi \sim 0$ while $\varphi \to 1$ for the ordered phase. A critical line $\eta_c(v_0, \rho)$ separates the disordered from the ordered states. To ensure the independence from initial conditions, φ has to be averaged over time after it reaches a stationary regime. This value is called φ_{stat}. The order of this phase transition is still a matter of controversy [10,11]. Until now the consensus seems to indicate that depending on how the noise is applied—angular noise or vectorial noise—the transition can be continuous or first-order like, respectively (for more details, see Ref. [2]).

B. The social force model

Contemporary to the VM, the *social force model* (SFM) was proposed by Helbing and Molnar [5,12] to describe the behavior of pedestrians. Since then, the SFM has been widely studied and applied for different situations (see, for example, Refs. [6,13,14]).

The SFM determines the direction of motion for each particle by taking into account three interactions: the "desire force," the "social force," and the "granular force," which are defined as

(1) The "desire force" ($\mathbf{F_{Di}}$) represents the desire of SPP to march in a given direction; if we are modeling the evacuation of a crowd, the target of the desire will be the exit. This force involves the idea of a desired speed of motion v_D, and it is given by

$$\mathbf{F_{Di}} = m_i \frac{(v_D \hat{\mathbf{e}}_\mathbf{t} - \mathbf{v_i})}{\tau_{\text{RT}}}, \tag{5}$$

where m_i is the particle mass, $\mathbf{v_i}$ is the current particle velocity, $\hat{\mathbf{e}}_\mathbf{t}$ the unit vector pointing to the target direction, and τ_{RT} is the relaxation time of the particle velocity toward v_D. In the present work, the desired speed has been taken as equal to the Vicsek-particle speed $v_D = v_0$.

(2) The "social force" ($\mathbf{F_{Si}}$) takes into account the fact that people like to move without bodily contact with other individuals. The "private space" wish is represented as a short range repulsive force based on the distance $r_{ij} = \|\mathbf{r_i} - \mathbf{r_j}\|$ between the center of mass of the individual i and its neighbor j. The complete expression is the following:

$$\mathbf{F_{Si}} = \sum_{j(\neq i)}^{N} A \exp\left[\frac{(d - r_{ij})}{B}\right] \hat{\mathbf{n}}_{\mathbf{ij}}, \tag{6}$$

where the constants A and B (assumed to be the same for all particles) define the strength and range of the social force, $\hat{\mathbf{n}}_{\mathbf{ij}}$ is the normalized vector pointing from pedestrian j to i, and d is the pedestrian diameter when one considers identical particle sizes.

(3) The "granular force" ($\mathbf{F_{Gi}}$) is considered when the pedestrians are in contact with each other. It is a repulsive force inspired by granular interactions, includes compression and friction terms, and is expressed as

$$\mathbf{F_{Gi}} = \left[k\ \hat{\mathbf{n}}_{\mathbf{ij}} + \kappa \Delta v^t_{ji}\ \hat{\mathbf{t}}_{\mathbf{ij}}\right] g(d - r_{ij}), \tag{7}$$

where $g(d - r_{ij})$ is zero when $d < r_{ij}$ and $d - r_{ij}$ otherwise. The first term represents a compressive force, its strength given by the constant k, which acts in the $\hat{\mathbf{n}}_{\mathbf{ij}}$ direction. The second term in Eq. (7)—related to friction—acts in the tangential direction $\hat{\mathbf{t}}_{\mathbf{ij}}$ (orthogonal to $\hat{\mathbf{n}}_{\mathbf{ij}}$), and it depends on the difference $\Delta v^t_{ji} = (\mathbf{v_j} - \mathbf{v_i}) \cdot \hat{\mathbf{t}}_{\mathbf{ij}}$ multiplied by the constant κ.

The interaction pedestrian—wall is defined analogously by means of social ($\mathbf{F_{SWi}}$) and granular forces ($\mathbf{F_{GWi}}$). If r_{iW} denotes the distance between the i-pedestrian and the wall, and $\hat{\mathbf{n}}_{\mathbf{iW}}$ is the wall normal pointing to the particle, then the "social force" is defined as

$$\mathbf{F_{SiW}} = A \exp\left[\frac{(d/2 - r_{iW})}{B}\right] \hat{\mathbf{n}}_{\mathbf{iW}}. \tag{8}$$

Similarly, denominating $\hat{\mathbf{t}}_{\mathbf{iW}}$ as the direction tangential (orthogonal to $\hat{\mathbf{n}}_{\mathbf{iW}}$), the "Granular force" is expressed as

$$\mathbf{F_{GWi}} = [k\ \hat{\mathbf{n}}_{\mathbf{iW}} - \kappa(\hat{\mathbf{v}}_{\mathbf{i}} \cdot \hat{\mathbf{t}}_{\mathbf{iW}})\ \hat{\mathbf{t}}_{\mathbf{iW}}] g(d/2 - r_{iW}). \tag{9}$$

For the force constants in the interactions between the particles and the walls we choose the same values as for the interparticle forces.

By considering all the forces described above, the equation of motion for pedestrian i of mass m_i is given by

$$\mathbf{v_i^{SFM}}(t + \Delta t) - \mathbf{v_i^{SFM}}(t) = \frac{1}{m_i}(\mathbf{F_{Di}} + \mathbf{F_{Si}} + \mathbf{F_{SWi}} + \mathbf{F_{Gi}} + \mathbf{F_{GWi}})\Delta t, \tag{10}$$

$$\mathbf{r_i}(t + \Delta t) = \mathbf{r_i}(t) + \mathbf{v_i^{SFM}}(t + \Delta t)\Delta t. \tag{11}$$

C. The combined model (SFM + VM)

Realistic evacuations in a nonpanic situation have different behavior depending on geometry and average speed. However, and even in the case of similar boundary conditions, it is expected that one observes differences between evacuations in a school, hospital, or airport. An important factor here is the existence of intrinsic fluctuations in the moving-interacting particles, such as children, passengers, or patients. Furthermore, humans display behavior not captured by the forces in the SFM. For instance, people would like to catch up with those walking (or running) in front of them and avoid being overrun by those behind, i.e., they are displaying velocity-dependent interactions beyond spatial ones. Both these effects can be included in the modeling by combining the standard SFM with the Vicsek model.

The central idea is to take into account not only the social interactions described above but the influence of nearest neighbors in the *Vicsek-style*, and to include noise η as an external parameter, which modulates this interaction. We will refer to this model as $SFM + VM$. In this way, in the SFM + VM the velocity of particle i is given by

$$\mathbf{v}_i(t + \Delta t) = v_0 \frac{\mathbf{v}_i^{VM}(t + \Delta t) + \Delta \mathbf{v}_i^{\mathrm{SFM}}(t)}{\left\| \mathbf{v}_i^{VM}(t + \Delta t) + \Delta \mathbf{v}_i^{\mathrm{SFM}}(t) \right\|}. \tag{12}$$

Here $\mathbf{v}_i^{VM}(t + \Delta t)$ is the velocity of particle i given by Eq. (2) and $\Delta \mathbf{v}_i^{\mathrm{SFM}}(t)$ is the velocity change of the SFM given by Eq. (10).

III. SIMULATION DETAILS

As was previously mentioned, we are going to compare all models under equal external conditions. An important point here is to match all relevant physical units in the models. To match the simulations to real systems, we have assumed length-units are given in meters and time-units, in seconds. To correlate pedestrians with particles, in the case of the SFM and SFM + VM, we have considered particles with $d = 0.7$ m (with $R_0 = 1$ m as the VM interaction range) and 80 kg of mass. We use the typical value $\tau_{\mathrm{RT}} = 0.5$ s for the relaxation time in the SFM and an integration time step of $\Delta t = 0.1$ s. This set of values allows us, on the one hand, to combine the (discrete) VM with the (continuous) SFM, and on the other hand, it yields a reliable discretization of the SFM dynamics.

After these assumptions, it is possible to define the mass and force variables in Eq. (10) as kilograms and Newtons, respectively, as the SFM requires.

The simulations were performed in a system of $N = 300$ self-propelled particles moving in corridor of size $L_x \times L_y$, with $L_x = 600$ and $L_y \in [2.5, 6]$. Periodic boundary conditions were applied in the horizontal direction at L_x, so that circulation of particles occurred in a loop. A size of $L_x = 600$ was then chosen to make sure that the fastest particles do not meet the stragglers.

The characteristic parameters of SFM interactions [Eqs. (5)–(7)] have been taken from previous works [5,15], specifically $A = 2000$ N, $B = 0.08$ m, $k = 1.2 \times 10^5$ kg s^{-2}, and $\kappa = 2.4 \times 10^5$ kg/(m s). These values correspond to a typical crowd.

In every case studied, several tests have been performed to assure the reliability of the data, that are not shown here for the sake of space. We made sure that starting from different initial conditions of particle distribution in position and direction of motion, $\varphi(t)$ reached the same value in the stationary regime (φ_{stat}). Also, the run-to-run fluctuations in the $\varphi(t)$ profile were not drastic. To determine the number of reasonable runs for the simulations, a first study was made observing how the average value of φ_{stat} and its uncertainty varied according to how many runs were taken in the average. As a conclusion, we considered 50 runs for each set of simulation parameters.

As was mentioned, the VM is a simple model that does not take into account short-range interactions such as excluded-volume or friction between particles and with walls. Moreover, taking into account that the aim of this work is to analyze the collective motion of individuals moving through a corridor, we introduce a series of variations on the VM. On the one hand, we relaxed the standard periodic boundary

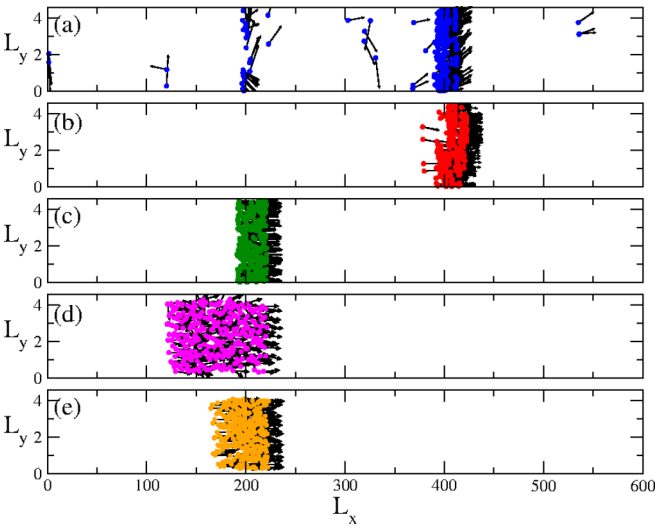

FIG. 1. Snapshots in the stationary-ordered state for $N = 300$, $L_x = 600$, $L_y = 4.5$ ($\rho = 1/9$), $\eta = 0.05$, $v_0 = 0.5$, and for different cases studied: (a) VM with periodic boundary conditions in the y direction (PBC); (b) VM with bouncing-back boundary condition in the y direction (BbBC); (c) VM + BbBc with a desired direction of motion (DD); (d) SFM + VM; and (e) SFM (in this case, the external noise η is not defined in the model). In all cases, PBC were applied in the x direction. (Color online: different colors link with data of Fig. 4.)

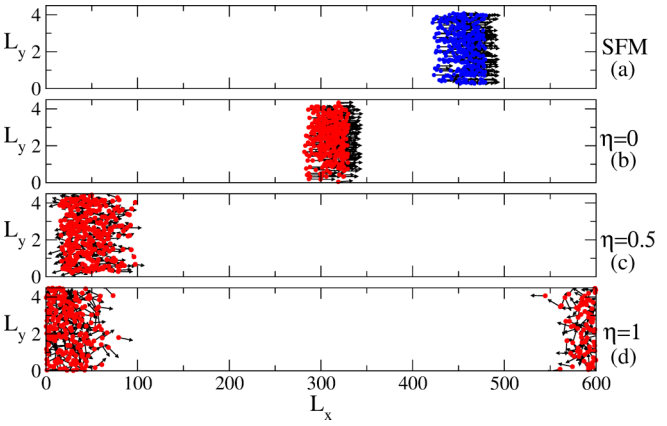

FIG. 2. Comparison of the stationary-state configurations for both (a) SFM and (b–d) SFM + VM for different external noise values η, as indicated. The snapshots correspond to $N = 300$, $L_x = 600$, $L_y = 4.5$ ($\rho = 1/9$), and $v_0 = 0.5$.

conditions (PBC) to a bouncing-back condition (BbC) in the y-direction. In this way, we simulate impenetrable walls at $y = 0$ and $y = L_y$, where particles rebound without losing energy.

On the other hand, we have introduced a *desired-direction* (DD) of motion, in such a way that the direction of motion at time $t + \Delta t$ given by Eq. (1) is modified by the addition of a desired-angle θ_{des} as

$$\tilde{\theta}_i(t + \Delta t) = \frac{\theta_i(t + \Delta t) + \theta_{\text{des}}}{2}, \tag{13}$$

with $\theta_{\text{des}} = 0$ in our case, indicating that particles prefer to move to the end of the corridor. This variation of the VM allows to introduce the existence of a preferred direction of motion, in the same sense as it is introduced in the SFM.

Finally, particles were inserted randomly in the first 0.5 L_x of the corridor with the intention to move toward the end of the corridor. The speed was considered in the range $v_0 = [0.5, 2]$ (m/s), consistent with normal evacuations in schools, hospitals, cinemas, etc.

For this reason, we have explored the range of $L_y \in [2.5, 6]$ (m) to represent the typical widths of corridors.

IV. RESULTS AND DISCUSSION

A full set of simulations was performed by taking into account the considerations mentioned above. In Fig. 1 we show several snapshots of stationary configurations in the ordered phase for all models with the same external parameters ($\eta = 0.05$—except for the SFM—and $v_0 = 0.5$) and different boundary conditions.

As can be seen, in the VM [Figs. 1(a)–1(c)], stationary-ordered-states correspond to the existence of bands perpendicular to the direction of motion. This fact has been widely studied and reported in the literature (see Refs. [2,3], and reference therein). However, it is worth to mention that different boundary conditions seem to affect the local order within the band of particles [e.g., PBC in Fig. 1(a) in comparison with BbBC in Fig. 1(b)]. For the VM cases, the most ordered configuration corresponds to the VM + BbBC + DD [Fig. 1(c)], as it is expected. Here, the incorporation of a preferential direction of motion can be interpreted as an external field applied in the system promoting order. However, in both SFM + VM at low noise [Fig. 1(d)] and SFM [Fig. 1(e)], particles are ordered in a horizontal cluster configuration trying to keep a distance between each other and with the walls.

The similarity in behavior observed in snapshot configurations between low noise SFM + VM [Fig. 1(d)] and SFM [Fig. 1(e)] is broken when the noise η increases. This is explicitly observed in Fig. 2, where, as it is expected, disorder increases with noise η. In fact, it seems that at $\eta = 0.5$ [Fig. 2(c)] disorder in the system is maximum, while at $\eta = 1$ [Fig. 2(d)] particles block each other (this effect will be analyzed in detail below).

To appreciate in detail the influence of Vicsek interactions on the spatial configuration in the SFM, we have studied the evolution of particle clusters for several noise strengths. For this purpose, we define the density profile in the x direction as

$$\text{P}(x, t) = \frac{\text{Number of particles between } x \text{ and } x + \Delta x}{N}, \tag{14}$$

and consequently $\text{P}(x, t)$ can be interpreted as a histogram, with bins of width Δx. In our case, we have fixed $\Delta x = 5 \gg d = 0.7$ so that we have the chance to find many particles in the bin. The size of the bin is such that it is not too small to allow the cluster to be described as continuous (no empty bins in the middle) but also not so large that it cannot be appreciated how the size changes over time.

In this way, the width of the density profile at time t ($w(t)$) can be defined as the distance between the maximum and the minimum values of x for which $P(x, t) > 1/N$, properly

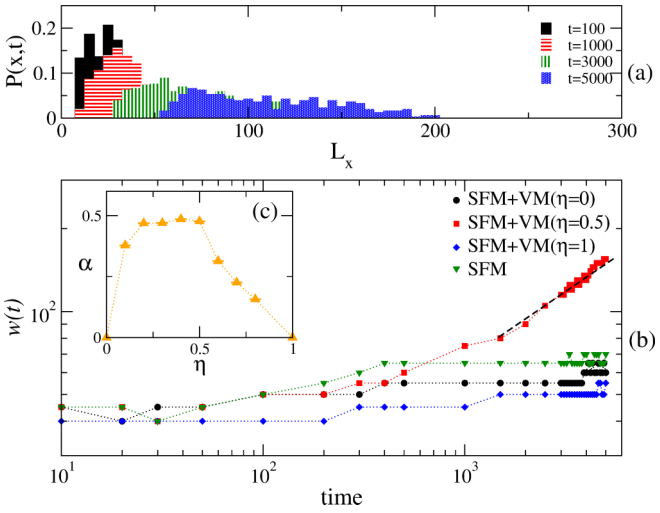

FIG. 3. (a) Density profile of the SFM + VM for $\eta = 0.5$. (b) Log-log plot of the cluster width $w(t)$ versus time for different noise strengths as indicated. The segmented lines represent the fits to the points proposing a power-law behavior with exponent α. (c) α as a function of noise η in the case of SFM + VM. α rises to ≈ 0.5 when the noise increases from $\eta = 0.1$ to $\eta = 0.5$, and then it decays to zero. The data presented in the figures correspond to simulation parameters $N = 300$, $L_x = 600$, $L_y = 4.5$ ($\rho = 1/9$), and $v_0 = 0.5$.

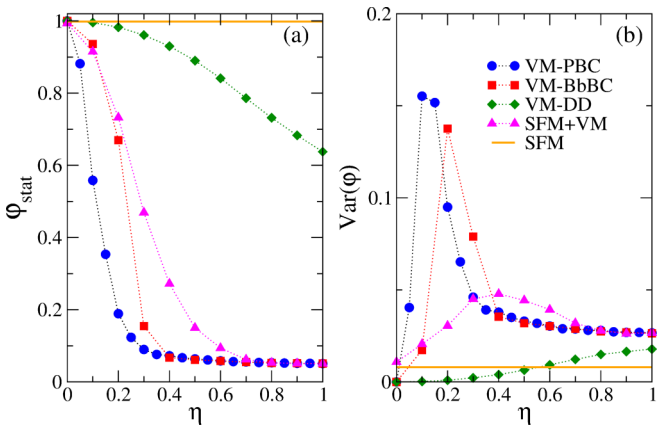

FIG. 4. (a) Order Parameter φ_{stat}, and (b) variance Var(φ), as a function of external noise η, for $N = 300$, $L_x = 600$, $L_y = 4.5$, $v_0 = 0.5$, and different models studied, as indicated.

normalized by considering the PBC applied in the x-direction. With this idea, $w(t)$ is directly associated with the extension of the cluster of particles as a function of time.

The obtained results show that at low noise the stationary cluster keeps its form and $w(t)$ is constant in time. However, when the noise increases particles spread and therefore the cluster width grows with time. This effect is most relevant for $\eta = 0.5$. The dynamic dependence of $w(t)$ [Fig. 3(b)] suggests a power-law behavior of the form

$$w(t) \propto t^{\alpha}, \tag{15}$$

where α has a strong dependence on noise. In fact, a least-squares fit of the data gives $\alpha \approx 0$ for $\eta = 0$ and the SFM, when external noise is increased $\alpha \to \frac{1}{2}$ for $\eta = [0.2, 0.5]$, and it monotonously diminishes to zero for $\eta = 1$. The alpha value observed in the $\eta = [0.2, 0.5]$ range is compatible with a diffusivelike spread of the particle front with the typical Einstein exponent $\alpha = \frac{1}{2}$. For higher noise it seems that the competition between random movement (given by the noise) and social-force interactions gives as a result a subdiffusive behavior with $0 < \alpha < \frac{1}{2}$. The behavior observed for $\eta = 1$ (see also Fig. 2(d)] is reminiscent of the *freezing by heating* effect observed in the SFM in the panic-regime [16,17]. In this case, the existence of increasing fluctuations in the system, or *nervousness of pedestrians*, produces a blocking effect and when they are in a disordered state particles can not move in the desired direction of motion.

Let us now turn to the question of an underlying nonequilibrium phase transition in the different models as a function of the noise strength by evaluating the stationary state φ_{stat} and its variance $\text{Var}(\varphi) \equiv \langle \varphi^2 \rangle - \langle \varphi \rangle^2$. Even in a d-dimensional nonequilibrium system, it is possible to relate fluctuations of the order parameter with a finite-size susceptibility as $\chi \equiv L^d \text{Var}(\varphi)$ [18].

The dependence of both quantities (φ_{stat} and Var(φ)) as a function of η for fixed speed ($v_0 = 0.5$) and lattice size ($L_x \times L_y = 600 \times 4.5$) can be observed in Fig. 4. As a first comment, it should be noted that the application of BbBC seems to move the VM transition [maximum Var(φ) in Fig. 4(b)] to higher values of η in comparison with the PBC. This is in agreement with the snapshots of Figs. 1(a) and 1(b); at a given noise ($\eta < \eta_c$) the PBC case is more disordered than the BbBC one. Even when in both cases the stripe geometry confines particle movement, the existence of impenetrable walls in the BbBC increases significantly the confinement effects, and therefore it is expected that VM-alignment should be more relevant than for PBC.

The application of a desired direction of motion (DD) in the VM has substantially different consequences. Unlike in the standard VM (with both PBC and BbBC), VM + DD prevents the existence of a disordered phase as it is expected. This appears reflected in the fact that $\varphi_{\text{stat}} \nrightarrow 0$, and Var($\varphi$) is maximal when $\eta \to 1$.

In the case of the SFM + VM the presence of an external noise clearly modifies the behavior of motion in comparison with the SFM in a nonpanic regime in a corridor (when trivially one expects $\varphi_{\text{stat}} = 1$). Because in the SFM + VM repulsive interactions between particles make the formation of a condensed cluster more difficult, it is observed that $\varphi_{\text{stat}}^{\text{VM+DD}} > \varphi_{\text{stat}}^{\text{SFM+VM}}$ for every η. The existence of a maximum in Var(φ) [Fig. 4(b)] suggests to analyze the dependence of this behavior on external noise upon a variation of speed v_0 and system size $L_x \times L_y$. To check the reliability of the SFM + VM outcomes, we have performed the same analysis for the VM cases, where the Var(φ) maximum is related to the existence of a phase transition.

Our results are shown in Fig. 5. As can be seen, in the VM [Figs. 5(a) and 5(b)] the peak of the susceptibility $\chi = (L_x L_y)\text{Var}(\varphi)$ becomes narrower and higher as both N and system size are increased. This behavior is not observed in the case of VM + DD [Fig. 5(c)], as expected. In the case of the SFM + VM the—rounded—peak of χ as a function of η increases in height as N and the system size grow; however, it

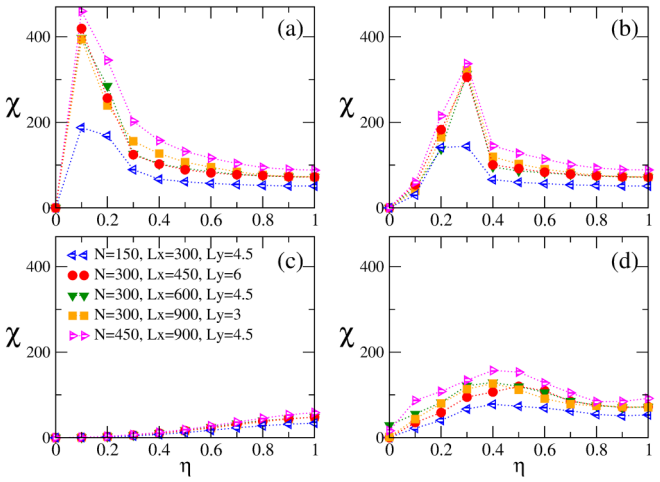

FIG. 5. $\chi = (L_x L_y)\mathrm{Var}(\varphi)$ as a function of noise η for fixed density $\rho = 1/9$, $v_0 = 0.5$, and different system size $L_x \times L_y$ and number of particles N, as indicated for (a) VM with PBC, (b) VM with BbBC, (c) VM with BbBC and desired direction of motion (DD), and (d) SFM + VM.

sharpens only very slowly. This could indicate an underlying phase transition but to clearly establish its existence it would be necessary to study much larger system sizes at fixed density than is possible within the scope of the present work. However, it is noteworthy that although the effect of external noise η in the model is less important than in the VM, it seems enough to break the symmetry imposed by SFM interactions.

Similar behavior is observed for the dependence of χ on speed v_0 (see Fig. 6). The susceptibility maximum diminishes as the speed increases, and its position seems to move to $\eta = 1$ for larger v_0. As can also be seen in this figure, for a given speed v_0 the maximum values of χ are higher in the case of the VM + BbBC than the SFM + VM.

Additionally, substantial information can be gleaned from level plots of φ_{stat} for several L_y values and noise values in the range 0–0.6 (Fig. 7). Because in these plots we are keeping N and L_x fixed, the vertical axis L_y is an indirect

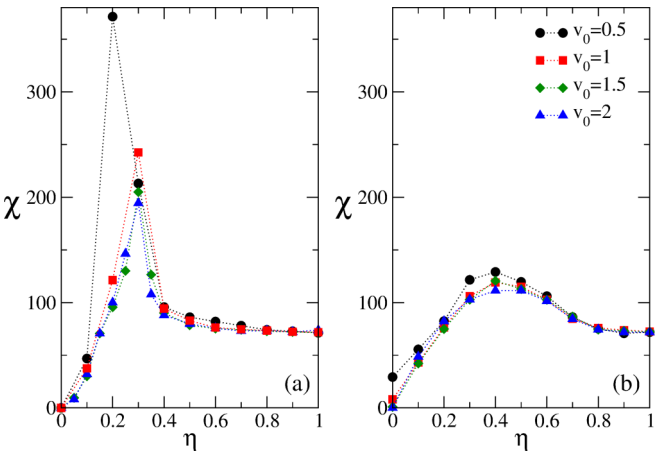

FIG. 6. $\chi = \mathrm{Var}(\varphi)(L_x L_y)$ as a function of noise η for $N = 300$, $L_x = 600$, $L_y = 4.5$ and different speeds v_0 as indicated. Cases are (a) VM with BbBC and (b) SFM + VM.

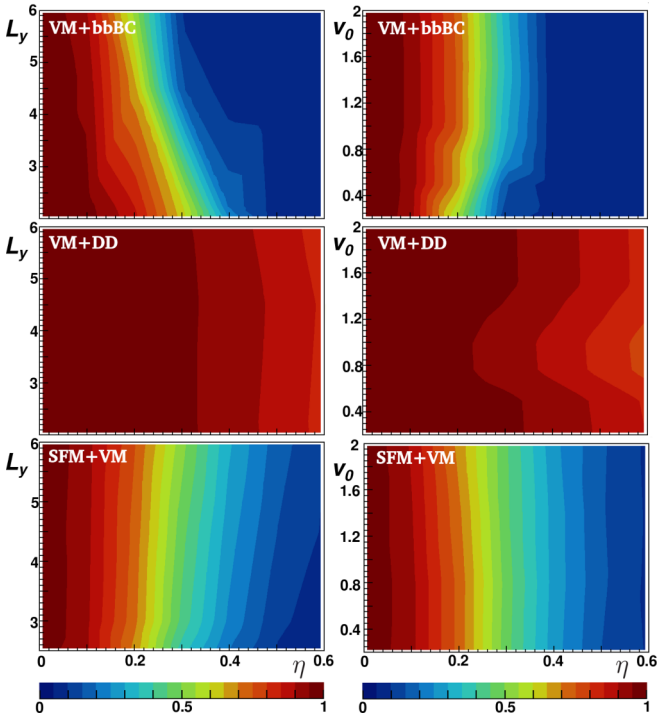

FIG. 7. Level plots of φ_{stat} for $N = 300$, $L_x = 600$ as a function of noise η (x axis). Left panel: for different densities (L_y variable and L_x fixed) for fixed speed $v_0 = 0.5$. Right panel: for different speeds v_0 at fixed $L_y = 4.5$ ($\rho = 1/9$).

representation of the density ρ. From these plots it can be appreciated that although the previous analysis was presented for a given value of ρ and v_0, similar behavior is observed for $\rho \in [\frac{1}{12}, \frac{1}{5}]$ and $v_0 \in [0.5, 2]$ (Fig. 7). In this way, our conclusions can be extended to a wide range of densities and speeds within the nonpanic regime.

V. COMPARISON WITH EXPERIMENTS

A great variety of experiments and real-life analysis have been carried out on pedestrian motion in corridor geometries (see, e.g., Refs. [19–21]). However, to quote from the introduction of [21]: "Despite the obvious importance of empirical data, it is surprising that no consensus about the correct quantitative description exists even for the simplest scenarios." The *fundamental diagram* (FD) of pedestrian flow—a relation between flux and density–has emerged as the most important tool to analyze pedestrian motion. We have therefore determined the FD for our model as the standard measure to compare model results with real data. To obtain the FD it is necessary to define the pedestrian flow rate $J_s = \Delta N/\Delta t$, where ΔN is the number of pedestrian crossing a fixed location in a discrete-time interval Δt, and $\rho_{\Delta V}$ is the local density measured as the total number of pedestrians in a volume $\Delta V = L_y \Delta x$ close to the flow measurement point ($\Delta x = 12$ in our case). We have built the FD considering that in our case the speed $v = v_0$ is constant. In Fig. 8 we show the results obtained for the SFM + VM in the stationary regime for $\eta = 0$ and different values of corridor width (L_y) and speed (v_0). Additionally, in the Inset of Fig. 8 we present the outcomes

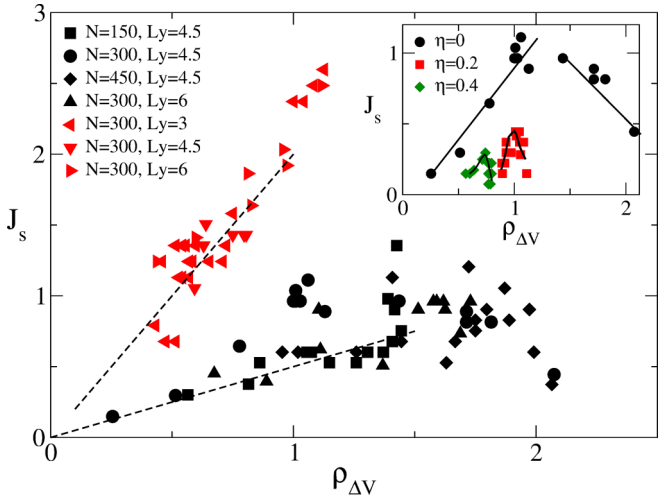

FIG. 8. J_s as a function of local density ρ_V, for different corridor widths L_y and number of particles N, as indicated, for the SFM + VM at $\eta = 0$. Black symbols correspond to $v_0 = 0.5$ and red ones to $v_0 = 2$. Dashed lines have slope $v_0\rho_{\Delta V}$. Inset: fundamental diagram for fixed $L_y = 4.5$, $v_0 = 0.5$, $N = 300$, and different noise values η as indicated. Full lines are to guide the eye.

considering several values of the external noise for fixed corridor width $L_y = 4.5$ and speed $v_0 = 0.5$. The results in the $\eta = 0$ case (nonpanic evacuation) are in good qualitative agreement with experimental data (see, e.g., Refs. [19–21]). A first increasing behavior of J_s as a function of local density is observed, and for $v_0 = 0.5$ a maximum is reached at $\rho_{\Delta V} \simeq 1.2$ beyond which the flux decreases again. At $v_0 = 2$ only the growing behavior is observed because at this speed the crowd is more extended, and therefore higher values of $\rho_{\Delta V}$ are unreachable in the stationary state at $\eta = 0$. Inclusion of noise, as in the inset, does not change the qualitative form of the FD but compressed it in the density direction and shifts the maximum to lower values of $\rho_{\Delta V}$ and a lower maximum flux.

VI. SUMMARY AND CONCLUSIONS

We have studied the role of interactions in the behavior of pedestrians moving in a corridorlike system. For this purpose, we have introduced a model that we have called SFM + VM, as a combination of both the well-known Vicsek and social force models. To check its performance, we have started our analysis with the Vicsek model in a confined geometry with different boundary conditions applied. In particular, we have studied the effects of bouncing-back boundary conditions that reproduce the effects of walls, and the existence of a desired direction of motion—the end of the corridor. We have compared these results to those obtained with the SFM and the SFM + VM.

Particle configurations in the ordered-steady-state are qualitatively different between the models analyzed. While in the VM, particles move in a more or less compact band perpendicular to the direction of motion, in the SFM and the SFM + VM particles exhibit some horizontal stripes parallel to the direction of motion. This effect is a consequence of the repulsive interactions between particles and with the walls present in those two models (Figs. 1 and 2). To compare both SFM and SFM + VM, we have analyzed the density-profile in the direction of motion (x) and determined its width as a function of time. Our results indicate that the width in the SFM + VM case has a power-law behavior with a dynamical exponent α, which depends on the external noise η. In particular, we have determined that $\alpha \approx 1/2$ at $\eta = [0.2, 0.5]$ and it monotonously approaches $\alpha = 0$ at $\eta = 1$ (Fig. 3). We have associated this change from an expected diffusivelike to a subdiffusive behavior to the competition between VM-like interactions and social interactions. At high noise, fluctuations have a *freezing by heating* effect, that has been reported only in the panic-regime before [16,17]. In our case, this effect appears in the system even at low-speed values, as a consequence of the introduction of the external noise, which therefore offers a means to introduce confusion or panic into evacuation models even at small speed of motion.

We have analyzed the order parameter φ, defined as the average velocity of the system, and its variance as function of external noise η for the diverse models described above (Figs. 4 and 5). In the VM, the application of different boundary conditions (periodic and bouncing-back) moves the critical value of the order-disorder phase transition to higher values of η. In contrast, the existence of a desired direction of motion in the VM promotes the order even at high values of external noise, annihilating the phase transition as expected. In the SFM + VM, the existence of an external noise that modulates the Vicsek-like interactions brakes the SFM symmetry (Fig. 6). As a consequence, both the order parameter and its variance are sensitive to this effect. Finally, we consider it important to remark that these outcomes can be observed in the whole range of densities $\rho \in [\frac{1}{12}, \frac{1}{9}]$ and speeds $v_0 \in [0.5, 2]$ studied, which encompass reasonable values of evacuations in a nonpanic regime (Fig. 7).

Based on these results and the comparison with real data (Fig. 8), we can conclude that the SFM + VM is a viable model to describe the pedestrian motion along a corridor in a nonpanic regime. It allows us to elucidate the role of the competition between social and alignment interactions, characteristics of the SFM and the VM, respectively.

In the SFM + VM, alignment interactions are tuned by the external noise η same as for the VM and this allows us to address questions on the existence of a nonequilibrium order-disorder transition controlled by this parameter. Our results are qualitatively compatible with the existence of such a transition, however, the approach to the thermodynamic limit seems to be very slow putting a final quantitative conclusion beyond the scope of this work.

ACKNOWLEDGMENTS

This work was supported by Consejo Nacional de Investigaciones Científicas y Técnicas (CONICET), Universidad Nacional de La Plata (Argentina), and Universidad Nacional de Quilmes (Argentina). Simulations were done on the cluster of *Unidad de Cálculo*, Instituto de Física de Líquidos y Sistemas Biológicos (IFLYSIB). We also thank Martin-Luther-University Halle-Wittenberg and Alexander von Humboldt Foundation for financial support.

[1] C. Castellano, S. Fortunato, and V. Loreto, Rev. Mod. Phys. **81**, 591 (2009).
[2] T. Vicsek and A. Zafeiris, Phys. Rep. **517**, 71 (2012).
[3] F. Ginelli, Eur. Phys. J. Special Topics **225**, 2099 (2016).
[4] T. Vicsek, A. Czirók, E. Ben-Jacob, I. Cohen, and O. Shochet, Phys. Rev. Lett. **75**, 1226 (1995).
[5] D. Helbing and P. Molnár, Phys. Rev. E **51**, 4282 (1995).
[6] D. Helbing and A. Johansson, Pedestrian, crowd, and evacuation dynamics, in *Extreme Environmental Events: Complexity in Forecasting and Early Warning*, edited by R. A. Meyers (Springer, New York, 2011), pp. 697–716.
[7] X. Chen, M. Treiber, V. Kanagaraj, and H. Li, Transport Reviews **38**, 625 (2018).
[8] D. S. Cambui, M. Godoy, and A. de Arruda, Phys. A **467**, 129 (2017).
[9] G. Baglietto and D. R. Parisi, Phys. Rev. E **83**, 056117 (2011).
[10] H. Chaté, F. Ginelli, G. Grégoire, and F. Raynaud, Phys. Rev. E **77**, 046113 (2008).
[11] G. Baglietto and E. V. Albano, Phys. Rev. E **80**, 050103(R) (2009).
[12] D. Helbing, Behav. Sci. **36**, 298 (1991).
[13] D. Helbing, I. Farkas, and T. Vicsek, Nature **407**, 487 (2000).
[14] D. Helbing, P. Molnár, I. J.Farkas, and K. Bolay, Environment and Planning B: Planning and Design **28**, 361 (2001).
[15] G. A. Frank and C. O. Dorso, Physica A **390**, 2135 (2011).
[16] D. Helbing, I. J. Farkas, and T. Vicsek, Phys. Rev. Lett. **84**, 1240 (2000).
[17] D. Helbing, I. J. Farkas, P. Molnar, and T. Vicsek, *Pedestrian and Evacuation Dynamics* (Springer, 2002), Vol. 21, p. 21.
[18] K. Binder and D. P. Landau, *A Guide to Montecarlo Simulations in Statistical Physics* (Cambridge University Press, Cambridge, UK, 2002).
[19] J. Zhang, W. Klingsch, A. Schadschneider, and A. Seyfried, J. Stat. Mech.: Theory Exp. (2011) P06004.
[20] S. Cao, A. Seyfried, J. Zhang, S. Holl, and W. Song, J. Stat. Mech.: Theory Exp. (2017) 033404.
[21] M. Boltes, J. Zhang, A. Tordeux, A. Schadschneider, and A. Seyfried, *Encyclopedia of Complexity and Systems Science* (Springer, Berlin, 2018), p. 1.